Internal ballistics model of recoilless weapons with moving high-pressure chambered

Do Quoc Vi[1], Do Van Minh[2], Tran Van Doanh[2], Nguyen Trang Minh[1*]

[1]Academy of Military Science and Technology, 17 Hoang Sam, Cau Giay, Hanoi, Vietnam;
[2]Faculty of Weapons, Le Quy Don Technical University, 246 Hoang Quoc Viet, Bac Tu Liem, Hanoi, Vietnam.
[*]Corresponding author: ngtrangminh@gmail.com
Received 6 Nov. 2024; Revised 3 Jan. 2025; Accepted 5 Feb. 2025; Published 25 Feb. 2025.
DOI: https://doi.org/10.54939/1859-1043.j.mst.101.2025.155-166

ABSTRACT

This paper presents an internal ballistics model for recoilless weapons with a high-pressure chamber, in which the chamber moves relative to the grenade. The model can also be applied to other scenarios, including a stationary high-pressure chamber, flowing out from high and low-pressure chambers, or a high-pressure chamber moving together with the grenade. The problem is solved using the numerical integration method in the MATLAB software. The maximum difference between the results of the mathematical model and experimental data was found to be 8.48% for both the case of a moving high-pressure chamber and a stationary chamber.

Keywords: Recoilless weapons; Interior ballistics; Moving high-pressure chamber.

1. INTRODUCTION

High-pressure chambered recoilless weapons (HPC-RW) are widely used due to their compact and lightweight design, offering high mobility. A key feature of these weapons is the separation of functions between chambers: the propellant burns in the high-pressure chamber, providing stable combustion, while the grenade remains in the low-pressure chamber, reducing mechanical stress on the grenade and barrel.

Existing studies on high-low pressure weapons have primarily focused on stationary high-pressure chambers [4, 6-10], successfully addressing internal ballistic characteristics under such conditions. However, these models neglect the dynamics of a moving high-pressure chamber, which is critical for recoilless systems. The system of differential equations developed in [10] accounts for factors such as initial propellant temperature, ignition tube combustion, gas exchange between chambers, and leakage through the grenade-barrel gap. This system was validated through experiments for two initial temperatures (5 °C and 50 °C), with errors between theoretical and experimental results staying below 10%.

Building on the theoretical framework from [10], this paper develops a generalized internal ballistic model for HPC-RW that incorporates the independent movement of the high-pressure chamber. This model can accommodate various scenarios, including stationary HPCs, high- and low-pressure gas flow, and synchronized movement of the HPC with the grenade. The model was validated experimentally, with results showing a maximum deviation of 8.48% for both moving and stationary HPC cases, highlighting its reliability and broader applicability.

2. THEORETICAL MODEL

2.1. Principle of operation of recoilless weapons with moving high-pressure chambered

A schematic illustration of the internal ballistic cycle of a recoilless weapon with a moving high-pressure chamber is shown in figure 1.

The internal ballistic cycle begins with the ignition of the charge in the ignition tube. The fuse burns at a constant volume until the gas pressure reaches a value at which the seal is broken. When the vents are opened, the propellant gas flows into the high-pressure chamber and ignites the

propellant charge. The propellant gas burns in a constant volume of the high-pressure chamber until the gas pressure in the high-pressure chamber reaches the pressure value of nozzles 1, 2, and 3, respectively. In this order, nozzles 1, 2, and 3 are disconnected. The propellant gas flows into the low-pressure chamber through nozzle 1 and into the atmosphere through nozzles 2 and 3.

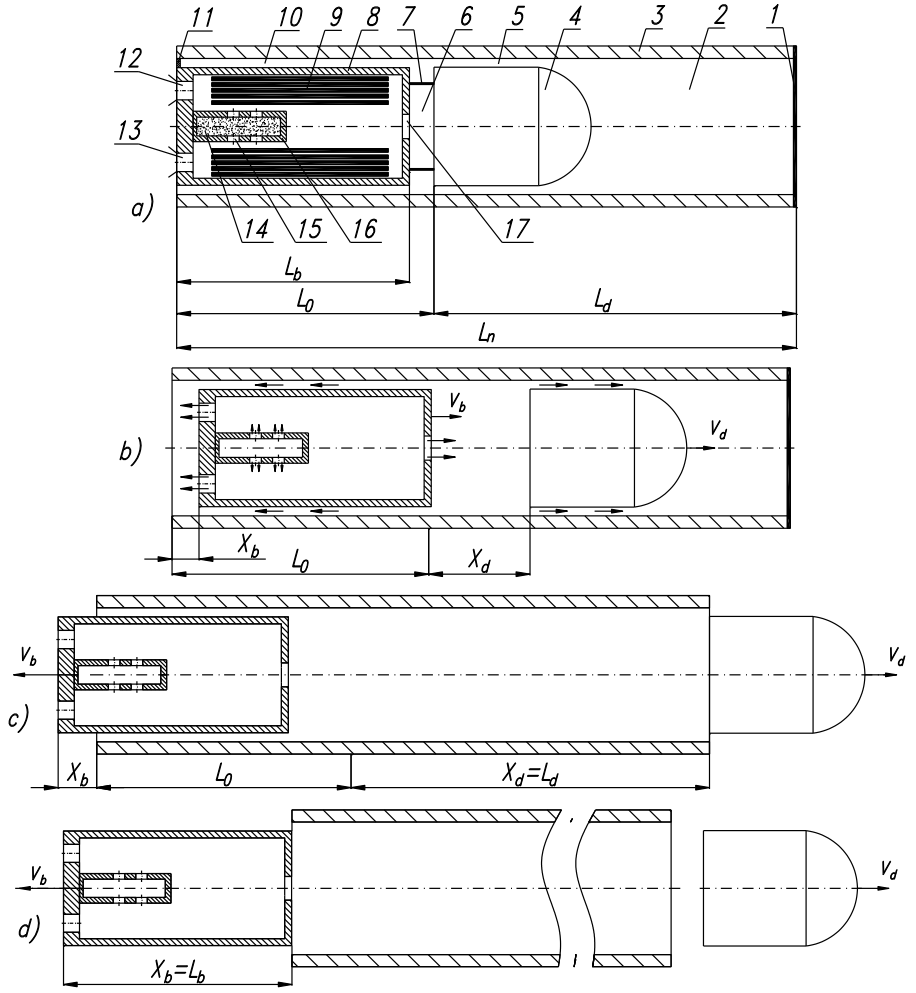

Figure 1. *The scheme of a recoilless weapon with moving high-pressure chambered.*
1. Cap; 2. Chamber N.4; 3. Barrel; 4. Grenade; 5. The gap between barrel and grenade;
6. Low-pressure chamber; 7. Joint 1; 8. High-pressure chamber; 9. Propellant;
10. The gap between barrel and HPC; 11. Joint 2; 12. Nozzle 2; 13. Nozzle 3;
14. Igniter charge; 15. Vents; 16. Igniter tube; 17. Nozzle 1.
a) t = 0, Initial time; b) Grenade and HPC are moving inside the barrel;
c) Grenade exits the barrel while HPC is still moving inside the barrel;
d) Both the grenade and HPC have exited the barrel.

The propellant gas from the low-pressure chamber will leak through the gap between the grenade and the barrel, between the HPC and the barrel. When the gas pressure in the low-pressure chamber reaches the critical value, it will release joint 1, pushing the grenade forward and creating its initial velocity. Conversely, if the connection between the HPC and the barrel (Joint 2) is broken, the HPC will also begin to move (if the connection remains intact, the HPC will stay stationary). Depending on the force acting on the HPC, it may move forward or backwards, exiting the barrel either before or after the grenade.

2.2. Mathematical model

The system of differential equations for the recoilless weapon in the case of a stationary HPC has been built by [10], based on fundamental assumptions [1-6, 8, 9]:

$$\frac{dz_1}{dt} = \frac{\left[1 - k_{t1}(T_{bd} - T_{tc1})\right]^{-1}}{I_{k1}} p_1 \tag{1}$$

$$\frac{d\psi_1}{dt} = \chi_1 \left(1 + 2\lambda_1 z_1 + 3\mu_1 z_1^{\,2}\right) \frac{dz_1}{dt} \tag{2}$$

$$\frac{dm_{g1}}{dt} = \omega_1 \frac{d\psi_1}{dt} - \frac{dm_{flv}}{dt} \tag{3}$$

$$\frac{dm_{flv}}{dt} = \begin{cases} \dfrac{\varphi_{2v} S_v p_1}{\sqrt{f_1 \tau_1}} K_0 & ,if\ \dfrac{p_1}{p_2} \geq k_{crit} \\ \dfrac{\varphi_{2v} S_v p_1}{\sqrt{f_1 \tau_1}} \sqrt{\dfrac{2k_0}{k_0 - 1}\left[\left(\dfrac{p_2}{p_1}\right)^{\frac{2}{k_0}} - \left(\dfrac{p_2}{p_1}\right)^{\frac{k_0+1}{k_0}}\right]} & ,if\ 1 < \dfrac{p_1}{p_2} < k_{crit} \\ -\dfrac{\varphi_{2v} S_v p_2}{\sqrt{f_2 \tau_2}} K_0 & ,if\ \dfrac{p_2}{p_1} \geq k_{crit} \\ -\dfrac{\varphi_{2v} S_v p_2}{\sqrt{f_2 \tau_2}} \sqrt{\dfrac{2k_0}{k_0 - 1}\left[\left(\dfrac{p_1}{p_2}\right)^{\frac{2}{k_0}} - \left(\dfrac{p_1}{p_2}\right)^{\frac{k_0+1}{k_0}}\right]} & ,if\ 1 < \dfrac{p_2}{p_1} < k_{crit} \\ 0 & ,if\ p_1 = p_2 \end{cases} \tag{4}$$

$$\frac{d\tau_1}{dt} = \begin{cases} \dfrac{(1-\tau_1) f_1 \omega_1 \dfrac{d\psi_1}{dt}}{f_1 m_{g1}}, \ if\ p_1 \geq p_2 \\ \dfrac{(1-\tau_1) f_1 \omega_1 \dfrac{d\psi_1}{dt} - (f_2\tau_2 - f_1\tau_1)\dfrac{dm_{flv}}{dt}}{f_1 m_{g1}}, \ if\ p_1 < p_2 \end{cases} \tag{5}$$

$$p_1 = \frac{f_1 \tau_1 m_{g1}}{W_{01} - \dfrac{\omega_1}{\delta_1}(1 - \psi_1) - \alpha_1 m_{g1}} \tag{6}$$

$$\frac{dz_2}{dt} = \frac{\left[1 - k_{t2}(T_{bd} - T_{tc2})\right]^{-1}}{I_{k2}} p_2 \tag{7}$$

$$\frac{d\psi_2}{dt} = \chi_2 \left(1 + 2\lambda_2 z_2 + 3\mu_2 z_2^{\,2}\right) \frac{dz_2}{dt} \tag{8}$$

$$\frac{dm_{fl1}}{dt}=\begin{cases}\dfrac{\varphi_{21}S_1p_2}{\sqrt{f_2\tau_c}}K_0, & if\ \dfrac{p_2}{p_3}\geq k_{crit}\\ \dfrac{\varphi_{21}S_1p_2}{\sqrt{f_2\tau_c}}\sqrt{\dfrac{2k_0}{k_0-1}\left[\left(\dfrac{p_3}{p_2}\right)^{\frac{2}{k_0}}-\left(\dfrac{p_3}{p_2}\right)^{\frac{k_0+1}{k_0}}\right]}, & if\ 1<\dfrac{p_2}{p_3}<k_{crit}\\ -\dfrac{\varphi_{21}S_1p_3}{\sqrt{f_2\tau_t}}K_0, & if\ \dfrac{p_3}{p_2}\geq k_{crit}\\ -\dfrac{\varphi_{21}S_1p_3}{\sqrt{f_2\tau_t}}\sqrt{\dfrac{2k_0}{k_0-1}\left[\left(\dfrac{p_2}{p_3}\right)^{\frac{2}{k_0}}-\left(\dfrac{p_2}{p_3}\right)^{\frac{k_0+1}{k_0}}\right]}, & if\ 1<\dfrac{p_3}{p_2}<k_{crit}\\ 0, & if\ p_2=p_3\end{cases} \tag{9}$$

$$\frac{dm_{fl2}}{dt}=\begin{cases}\dfrac{\varphi_{22}S_2p_2}{\sqrt{f_2\tau_2}}K_0, & if\ \dfrac{p_2}{p_{kk}}\geq k_{crit}\\ \dfrac{\varphi_{22}S_2p_2}{\sqrt{f_2\tau_2}}\sqrt{\dfrac{2k_0}{k_0-1}\left[\left(\dfrac{p_a}{p_2}\right)^{\frac{2}{k_0}}-\left(\dfrac{p_a}{p_2}\right)^{\frac{k_0+1}{k_0}}\right]}, & if\ 1<\dfrac{p_2}{p_{kk}}<k_{crit}\end{cases} \tag{10}$$

$$\frac{dm_{fl3}}{dt}=\begin{cases}\dfrac{\varphi_{23}S_3p_2}{\sqrt{f_2\tau_2}}K_0, & \text{if}\ \dfrac{p_2}{p_a}\geq k_{crit}\\ \dfrac{\varphi_{23}S_3p_2}{\sqrt{f_2\tau_2}}\sqrt{\dfrac{2k_0}{k_0-1}\left[\left(\dfrac{p_a}{p_2}\right)^{\frac{2}{k_0}}-\left(\dfrac{p_a}{p_2}\right)^{\frac{k_0+1}{k_0}}\right]}, & \text{if}\ 1<\dfrac{p_2}{p_a}<k_{crit}\end{cases} \tag{11}$$

$$\frac{dm_{g2}}{dt}=\omega_2\frac{d\psi_2}{dt}-\frac{dm_{fl1}}{dt}-\frac{dm_{fl2}}{dt}-\frac{dm_{fl3}}{dt} \tag{12}$$

$$\frac{d\tau_2}{dt}=\begin{cases}\dfrac{(1-\tau_2)\omega_2\dfrac{d\psi_2}{dt}}{m_{g2}}, & if\ p_2\geq p_3\\ \dfrac{(1-\tau_2)\omega_2\dfrac{d\psi_2}{dt}-(\tau_3-\tau_2)\dfrac{dm_{fl1}}{dt}}{m_{g2}}, & if\ p_2<p_3\end{cases} \tag{13}$$

$$p_2=\frac{f_2\tau_2m_{g2}}{\mathrm{W}_{02}-\dfrac{\omega_2}{\delta_2}(1-\psi_2)-\alpha_2m_{g2}} \tag{14}$$

$$\frac{dm_{g3}}{dt}=\frac{dm_{fl1}}{dt} \tag{15}$$

$$\frac{dm_{f\,\mathrm{lg}}}{dt}=\begin{cases}\dfrac{\varphi_{2g}S_g p_3}{\sqrt{f_2\tau_3}}K_0, & if\ \dfrac{p_3}{p_a}\geq k_{crit}\\ \dfrac{\varphi_{2g}S_g p_3}{\sqrt{f_2\tau_3}}\sqrt{\dfrac{2k_0}{k_0-1}\left[\left(\dfrac{p_a}{p_3}\right)^{\frac{2}{k_0}}-\left(\dfrac{p_a}{p_3}\right)^{\frac{k_0+1}{k_0}}\right]}, & if\ 1<\dfrac{p_3}{p_a}<k_{crit}\end{cases} \tag{16}$$

$$\frac{d\tau_3}{dt}=\begin{cases}\dfrac{(\tau_2-\tau_3)dm_{fl1}-\dfrac{k_0-1}{k_0 f_2}\varphi mvdv}{m_{g3}}, & if\ p_2\geq p_3\\ \dfrac{-\dfrac{k_0-1}{k_0 f_2}\varphi mvdv}{m_{g3}}, & if\ p_2<p_3\end{cases} \tag{17}$$

$$p_3=\frac{f_2\tau_3 m_{g3}}{\mathrm{W}_{03}-\alpha_2 m_{g3}+S_n X_d} \tag{18}$$

$$p_4=\begin{cases}\dfrac{p_a\mathrm{W}_{04}}{\mathrm{W}_{04}-S_n X_d}, & if\ p_4\leq p_{br}\\ p_a, & if\ p_4>p_{br}\end{cases} \tag{19}$$

$$\frac{dv}{dt}=\frac{S_d(p_3-p_4)}{\varphi m} \tag{20}$$

$$\frac{dX_d}{dt}=v \tag{21}$$

The following symbols are used in the preceding equation:

- χ_1, λ_1, μ_1 are the shape characteristics of powder grain; z_1 is the relative burnt thickness of grain; ψ_1 is the relative burnt igniter propellant mass; α_1, δ_1, ω_1 are the covolume, density, and mas of igniter charge; I_{k1} is the total impulse of propellant gas; f_1 is the specific energy of igniter charge; T_{bd}, T_{tc1} are initial temperature and standard temperature of igniter charge; S_v is total area of vents; p_1, p_2 are gas pressure in igniter tube and high-pressure chamber; φ_{2v} is correction factor; W_{01} is the initial volume of igniter tube.

- χ_2, λ_2, μ_2 are the shape characteristic parameters of the powder grain; z_2 is the relative burnt thickness of grain; ψ_2 is the relative burnt propellant mass; α_2, δ_2, ω_2 are the covolume, density, and mas of propellant charge; I_{k2} is the total impulse of propellant gas; f_2 is the specific energy of propellant; T_{bd}, T_{tc2} are initial temperature and standard temperature of propellant; p_3, p_a are gas pressure in the low-pressure chamber and atmospheric pressure; φ_{21}, φ_{22}, φ_{23} is the correction factor; W_{02} is the initial volume of the high-pressure chamber. S_1, S_2, and S_3 are the total critical areas of nozzle 1, nozzle 2, and nozzle 3, respectively.

- S_g denotes the leakage area between grenade and barrel; φ_{2g} is correction factor; W_{03}, W_{04} are the initial volumes of low-pressure chamber and chamber Nr.4 chamber; m is the grenade mass; φ is the coefficient of fictitious grenade mass; v is the grenade velocity; S_n, S_d are the cross-sectional area of barrel and grenade; X_d is the grenade path in barrel; p_{br} is the value of the pressure that will cause bursting of the cap.

The relative temperature of the gas in the igniter tube, high-pressure chamber and low-pressure chamber are given by:

$$\tau_1 = \frac{T_1}{T_{c1}}; \tau_2 = \frac{T_2}{T_{c2}}; \tau_3 = \frac{T_3}{T_{c2}}$$

where T_1, T_2, T_3 are the gas temperatures in the igniter tube, high-pressure and low pressure chamber; T_{c1}, T_{c2} are the basic propellant combustion temperatures of igniter charge and propellant.

To build a new internal ballistic model, which the high-pressure chamber moves relative to the grenade, some equations need to be modified and supplemented. The additional equations needed are equation of motion, equation of the applied force and equation of mass of the high-pressure chamber.

Equation of motion

$$\frac{dv_b}{dt} = \begin{cases} \dfrac{F_{HPC} + S_d(p_3 - p_4)}{\varphi(m_{HPC} + m + m_{fl1} - m_{f\,\mathrm{lg}})}, & \text{if } F_{j1} < F_{j1crit} \text{ and } F_{j2} \geq F_{j2crit} \\ \dfrac{F_{HPC}}{\varphi m_{HPC}}, & \text{if } F_{j1} \geq F_{j1crit} \end{cases} \tag{22}$$

$$\frac{dX_b}{dt} = v_b \tag{23}$$

Equation of the applied force

$$F_{HPC} = \left(C_{p2}S_2 + C_{p3}S_3 - S_1\right)p_2 - \left(S_{HPC} - S_1\right)p_3 \tag{25}$$

$$C_{p2} = \varphi_{12}\varphi_{22}K_0F_{w2}(\xi_{a2}, k_0) \tag{26}$$

$$C_{p3} = \varphi_{13}\varphi_{23}K_0F_{w3}(\xi_{a3}, k_0) \tag{27}$$

Equation of mass

$$m_{HPC} = m_{HPC0} - m_{fl1} - m_{fl2} - m_{fl3} \tag{28}$$

The following symbols are used in the preceding equation: F_{HPC}, m_{HPC} are the applied force and mass of HPC; m_{HPC0} is the initial mass of HPC; S_{HPC} is the cross-sectional area of HPC; C_{p2}, C_{p3} are thrust coefficient of the nozzles 2, 3; F_{j1}, F_{j1crit} are force acting on the joint 1 and the value of force breaking the joint 1. F_{j2}, F_{j2crit} are force acting on the joint 2 and the value of force breaking the joint 2.

Modified equations:

$$\frac{dm_{g3}}{dt} = \frac{dm_{fl1}}{dt} - \frac{dm_{f\,\mathrm{lg}}}{dt} \tag{15'}$$

$$\frac{dm_{f\,\mathrm{lg}}}{dt} = \begin{cases} \dfrac{S_g p_3}{\sqrt{f_2\tau_3}}K_0, & \text{if } \dfrac{p_3}{p_a} \geq k_{crit} \\ \dfrac{S_g p_3}{\sqrt{f_2\tau_3}}\sqrt{\dfrac{2k_0}{k_0 - 1}\left[\left(\dfrac{p_a}{p_3}\right)^{\frac{2}{k_0}} - \left(\dfrac{p_a}{p_3}\right)^{\frac{k_0+1}{k_0}}\right]}, & \text{if } 1 \leq \dfrac{p_3}{p_a} < k_{crit} \end{cases} \tag{16'}$$

Where

$$S_g = \begin{cases} \varphi_{2d} S_{g1} + \varphi_{2b} S_{g2}, & \text{if } X_d \le L_d \text{ and } -L_b \le X_b \le L_n \\ \varphi_{2n} S_n, & \text{if } X_d > L_d \text{ or } X_b < -L_b \end{cases} \quad (29)$$

$$d\tau_3 = \frac{(\tau_{3i} - \tau_3) dm_{fl1} - \frac{k_0 - 1}{k_0 f_2} \varphi m v dv}{m_{g3}} \quad (17')$$

$$p_3 = \frac{f_2 \tau_3 m_{g3}}{W_{03} - \alpha m_{g3} + S_n (X_d - X_b)} \quad (18')$$

$$\frac{dv}{dt} = \begin{cases} \frac{F_{HPC} + S_d (p_3 - p_4)}{\varphi (m_{HPC} + m + m_{fl1} - m_{f\lg})}, & if\ F_{j1} < F_{j1crit} \text{ and } F_{j2} \ge F_{j2crit} \\ \frac{S_d (p_3 - p_4)}{\varphi m}, & if\ F_{j1} \ge F_{j1crit} \end{cases} \quad (20')$$

The following symbols are used in the preceding equation: L_d is the maximum distance travelled of the grenade within the barrel; X_b is the distance travelled within the barrel of HPC; L_b is the length of HPC; S_{g1}, S_{g2} denote the leakage area between the grenade and barrel, and between HPC and barrel.

3. RESULTS AND DISCUSSION

The system of equations that describes the new internal ballistic cycle consists of first-order ordinary differential equations and algebraic equations, from (1) to (29). In this system, equations (15), (16), (17), (18), (20) are modified into equations (15'), (16'), (17'), (18'), (20'). Using the fourth-order Runge-Kutta method, numerical integration software has been developed to determine the gas pressure changes in the igniter tube, high-pressure and low-pressure chamber, grenade velocity, and HPC velocity.

The above system of internal ballistic equations is applied to a 93 mm calibre recoilless gun, the design parameters of which are given in table 1.

Table 1. *Design parameter of recoilless weapon 93 mm.*

Parameters	Signification	Value	Parameters	Signification	Value
Caliber (m)	D	0.093	Propellant mass (kg)	ω_1	0.0145
Length of barrel (m)	L_n	0.9		ω_2	0.34
The maximum distance travel of grenade within the barrel	L_d	0.636	Specific energy of propellant (J/kg)	f_1	265035
Length of HPC (m)	L_b	0.19		f_2	857982
Cross-sectional area of barrel (m^2)	S_n	0.0068	Total pressure impulse of propellant gases (Pa.s)	Ik_1	$180x10^3$
Cross-sectional area critical of Nozzle (m^2)	S_1	$1.43x10^{-4}$		Ik_2	$350x10^3$
	S_2	$9.81x10^{-4}$	Geometric characteristics of powder grain	$\chi_1; \lambda_1; \mu_1$	3;-1;1/3
	S_3	$4.73x10^{-4}$		$\chi_2; \lambda_2; \mu_2$	1,036; 0,0036; 0

Parameters	Signification	Value	Parameters	Signification	Value
Total area of vents (m^2)	S_v	$8.03x10^{-5}$	Covolume of powder gas (m^3/kg)	$\alpha_1 = \alpha_2$	$1.24x10^{-3}$
Cross-sectional area gap between grenade and barrel (m^2)	S_{g1}	$3.36\ x10^{-5}$	Density of propellant (kg/m^3)	$\delta_1 = \delta_2$	1540
Cross-sectional area gap between HPC and barrel (m^2)	S_{g2}	$3.36\ x10^{-5}$	Specific heat ratio	k_0	1.22
Chamber initial volume (m^3)	W_{01}	$1.47x10^{-5}$	Grenade mass (kg)	m	3.94
	W_{02}	$6.04x10^{-4}$	Initial HPC mass (kg)	m_{HPC0}	2.48
	W_{03}	$4.47x10^{-4}$	Atmosphere pressure (Pa)	p_a	10^5
	W_{04}	$1.40x10^{-3}$	Initial temperature (^oC)	T_{bd}	5; 15; 50

The results of solution for the case of a moving high-pressure chamber and the initial temperature of the propellant is 15 ^{0}C are clearly shown in table 2 and figure 2.

Table 2. *The results of solution for the case of a moving high-pressure chamber.*

No.	At the moment	p_1 (MPa)	p_2 (MPa)	p_3 (MPa)	v (m/s)	X_d (m)	v_b (m/s)	X_b (m)	t (ms)
1	Maximum of p_1	178.15	4.17	0.17	0.01	-1.10^{-6}	0.20	$-1.6.10^{-5}$	0.70
2	Maximum of p_2	53.96	54.01	13.09	22.69	0.018	3.13	0.01	3.66
3	Maximum of p_3	51.04	51.05	14.50	36.42	0.037	0.85	0.01	4.29
4	Propellant burned out	35.49	35.50	6.16	114.89	0.471	8.85	0.01	9.60
5	Grenade exits barrel	5.68	5.11	4.88	126.45	0.636	1.95	0.02	10.97
6	HPC exits barrel	0.10	0.10	0.10	-	-	-10.97	-0.19	31.11

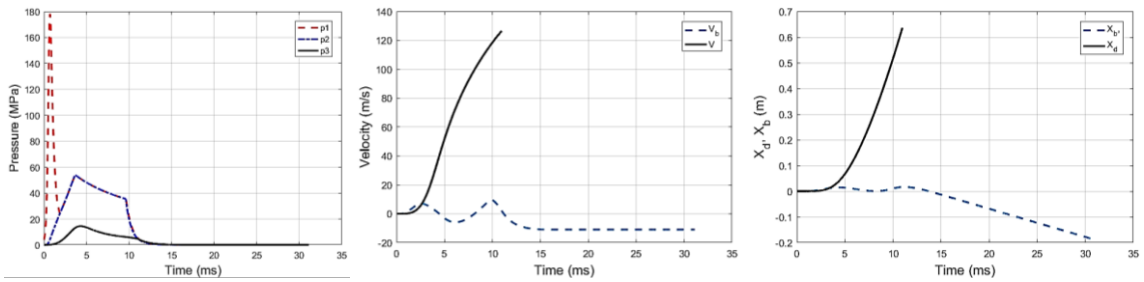

a) *b)* *c)*

Figure 2. *Pressure in the igniter tube, the high and low-pressure chamber plots vs time (a), the velocity of grenade and HPC plot vs time (b), the distance traveled within the barrel of grenade and HPC vs time (c).*

The results of the solution for the case of a stationary high-pressure chamber and the initial temperatures of the propellant are 5 ^{o}C, 15 ^{o}C, 50 ^{o}C are clearly shown in table 3, figure 3, 4.

Table 3. *The results of solution for the case of a stationary high-pressure chamber.*

No.	Parameters	5 ºC	15 ºC	50 ºC
1	p_{1max}, MPa	170.69	178.15	207.55
2	p_{2max}, MPa	53.90	54.01	59.02
3	p_{3max}, MPa	13.04	13.32	14.64
4	V_0, m/s	124.70	126.72	129.76

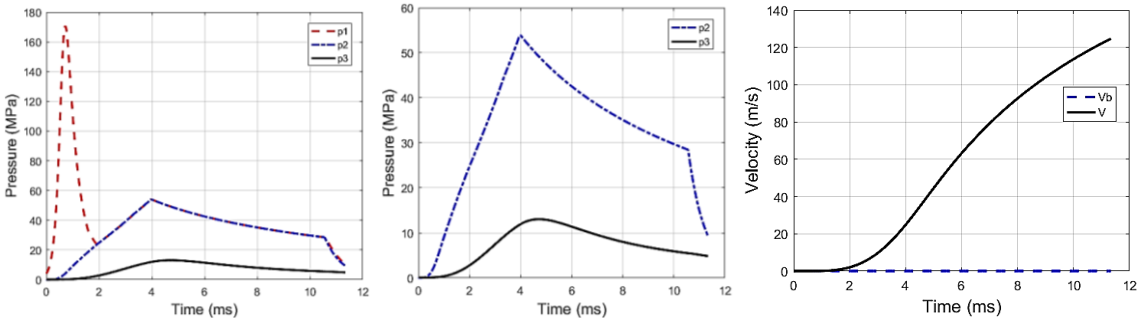

a) *b)* *c)*

Figure 3. *Pressure in the igniter tube, the high and low-pressure chamber plots vs time (a), (b), the velocity of grenade and HPC plot vs time (c) when temperature of the propellant is 5 ºC.*

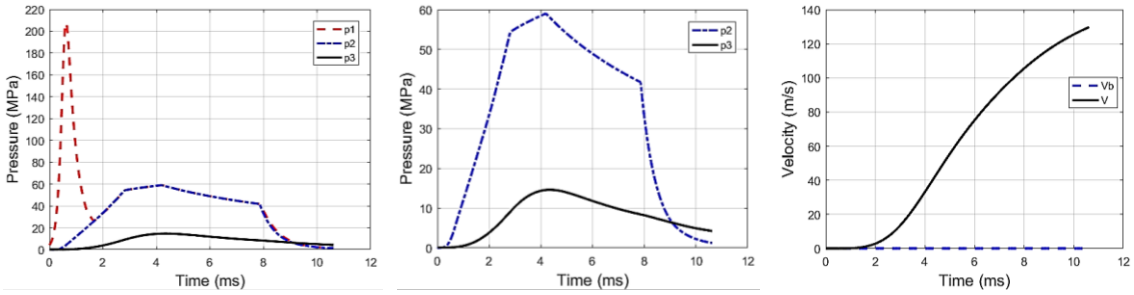

a) *b)* *c)*

Figure 4. *Pressure in igniter tube, high and low-pressure chamber plots vs time (a), (b), velocity of grenade and HPC plot vs time (c) when the temperature of the propellant is 50 ºC.*

To verify the mathematical model, the experiments were conducted, including the experiment for the case of a moving HPC (figure 5).

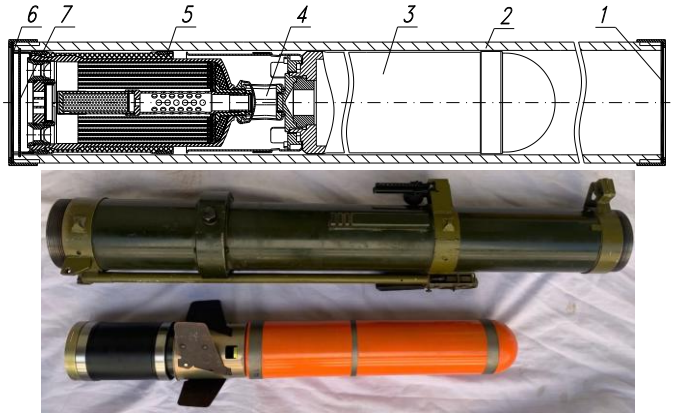

Figure 5. *The experimental setup for the case of a moving HPC.*

The test apparatus includes a firing tube (2), a cartridge with a high pressure chamber (5), a simulated grenade (3), caps (1, 6), a joint 1 (4), and a joint 2 (7). A high-speed camera Phantom

V711, which is located 20 m from the launcher system, was used to record the movement of the grenade and high pressure chamber, the chosen record rate was 2.000 frames per second. The flight time and distance of the grenade and high pressure chamber can be used to calculate the initial velocity. The temperature of the propellant before firing was 15 ^{o}C.

Table 4. *Experiment data for the case of a moving HPC.*

No.	v_0, m/s	v_{b0}, m/s	Δt, ms
1	126.8	11.3	25.1
2	127.6	10.8	25.7
3	128.7	11.3	23.6
4	125.4	12.6	21.2
5	126.8	11.1	26.7
6	128.5	13.7	26.2
7	128.5	12.6	24.3
Ave	**127.5**	**11.9**	**24.7**

The experiment results for the case of a moving HPC are presented in table 4 and figure 6.

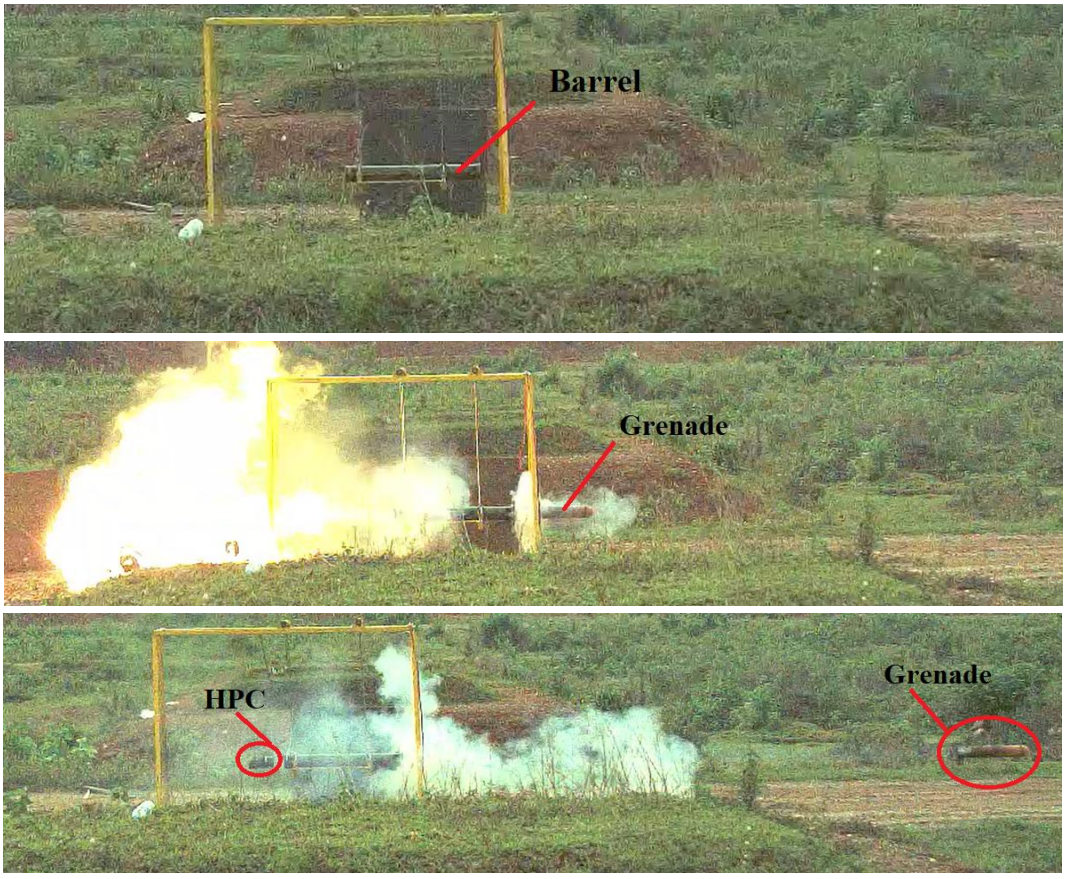

Figure 6. *The test video recording.*

Table 5 compares the values of velocity obtained by calculation and measurement. Table 6 compares the values of maximum shear pressure and velocity obtained by calculation and measurement. The experimental data and the calculation results are in good agreement, which indicates the accuracy of the algorithm.

Table 5. *The comparison of calculation and experiment results for the case of a moving HPC.*

TT	Parameters	Calculation	Experiment	Difference	Note
1	v_0, m/s	126.45	127.5	0.83%	
2	v_{b0}, m/s	-10.97	-11.9	8.48%	Backwards

Table 6. *The comparison of calculation and experiment results for the case of a stationary HPC.*

Parameters	Recalculation	Experiment [10]	Difference	Note
p_{2max}, MPa	53.90	49.99	7.25%	5 ^oC
p_{3max}, MPa	13.04	13.87	6.37%	
V_0, m/s	124.70	123.9	0,64%	
p_{2max}, MPa	59.02	58.66	0.61%	50 ^oC
p_{3max}, MPa	14.64	14.59	0.34%	
V_0, m/s	129.76	128.2	1.20%	

4. CONCLUSIONS

In this paper, an internal ballistic mathematical model was developed for recoilless weapons with a high-pressure chamber, where the chamber moves relative to the grenade. The model can also be applied to other cases, such as a stationary high-pressure chamber, flowing out from high and low-pressure chambers, or a high-pressure chamber moving together with the grenade. The problem was solved in the MATLAB environment.

The mathematical model and experiment were used to determine the gas pressure in the high-pressure chamber, low-pressure chamber, time, velocity of the grenade, and velocity of HPC, for both stationary and moving high-pressure chamber cases. Based on the results of the model, the experiments were carried out. By comparison, the difference between the result of the mathematical model and the value obtained by the experiment was found to be a maximum of 8.48%.

REFERENCES

[1]. Carlucci, D.E. and Jacobson, S.S,*"Theory and design of Guns and ammunition"*, Taylor & Francis, ISBN 9781315165967, (2018).

[2]. Plihal, B. Beer, S., Komenda, J., Jedlicka, L. and Kuda, B, *"Balistika",* Brno: University of Defence, ISBN 978-80-7231-785-1, (2011).

[3]. Plihal, B., Beer, S., Jedlicka, L,*"Interior ballistics of gun barrel: Collection of examples and exercises (in Czech)"*, Brno: University of Defence, (2005).

[4]. Bien,V.V, *"The Effect of The Nozzle Ultimate Section Diameter on Interior Ballistics of HV-76 Trial Gun"*, In International Conference on Military Technologies (ICMT), Brno: IEEE, (2019).

[5]. Doanh.V.T, *"Equation of energy of the internal ballistic model in the jet dynamic system",* Journal of Science and Technology, Le Quy Don Technical University, No. 151, (2012)

[6]. Jaramaz, S. Mickovic, D., Zivkovic,Z. and Curcic, R. *"Internal ballistic principle of high/low pressure chambers in automatic grenade launchers"*, in 19th International Symposium of Ballistics, Interlaken, Switzerland, (2001).

[7]. Vasile, T., Safta, D. and Barbu, C., *"Studies and researchers concerning grenade launcher with high-low pressure chambers"*, [online] [cited 2019-02-26], available from: https://www.researchgate.net/publication/267238161_Studies_and_researchers_concerning_grenade_launcher_with_high-low_pressure_chambers, (2019).

[8]. Dung.T.N, Linh.D.D, *"Internal ballistics of high-low pressure decoy launcher with a secondary propellant charge"*, In International Conference on Military Technologies (ICMT), Brno: IEEE, (2019).

[9]. Vi.D.Q, Minh.N.T, Minh.D.V, and Cuong.P.V, *"Building a model for the internal ballistic problem of recoilless weapons with high-pressure combustion chamber"*, Journal of Military Science and Technology, Academy of Military Science and Technology Vietnam, vol. 92, (2023).

[10]. Vi.D.Q, Minh.N.T, Minh.D.V, Dung.T.D, Macko Martin, Duc.L.M, Sy.N.T, Dung.B.V, *"Simulation of Internal Ballistics Calculation of High-Pressure Chambered Recoilless Weapons at Different Propellant Charge Temperature",* Advances in Military Technology, University of Defence, (2025).

TÓM TẮT

Mô hình thuật phóng trong của vũ khí không giật với buồng cao áp chuyển động

Bài báo này trình bày mô hình thuật phóng trong cho vũ khí không giật có buồng cao áp, trong đó buồng cao áp có chuyển động tương đối với đạn. Mô hình này cũng có thể được áp dụng cho các trường hợp khác, bao gồm buồng cao áp cố định, khí thoát ra từ buồng cao áp và thấp áp, hoặc buồng cao áp chuyển động cùng với đạn. Bài toán được giải quyết bằng phương pháp tích phân số trên phần mềm MATLAB. Sai số lớn nhất giữa kết quả của mô hình toán học và dữ liệu thực nghiệm là 8,48% đối với cả trường hợp buồng cao áp chuyển động và buồng cao áp cố định.

Từ khóa: Vũ khí không giật; Thuật phóng trong; Buồng cao áp chuyển động.